Composition dependence of the Γ_8-Γ_6 transition in mercury cadmium telluride: A reexamination

J. Camassel, J. P. Laurenti, and A. Bouhemadou
Groupe d'Etude des Semiconducteurs, Université des Sciences et Technique du Languedoc, 34060 Montpellier Cedex, France

R. Legros and A. Lusson
Laboratoire de Physique des Solides, Centre National de la Recherche Scientifique, 92190 Meudon, France

B. Toulouse
Laboratoire de Physique des Solides, Institut National des Sciences Appliquées, 35043 Rennes Cedex, France
(Received 24 December 1987; revised manuscript received 18 March 1988)

The composition dependence of the Γ_8-Γ_6 transition in mercury cadmium telluride (MCT) has long been classified apart among all disordered alloy systems. The nonconstant bowing parameter reported in this case could only be accounted for in terms of a finite departure from the virtual-crystal approximation but was not clearly reflected in the properties of carriers and/or the characteristics of the alloys. Moreover this nonconstant bowing appears to be a unique feature of MCT. First, it departs from all reports concerning standard II-VI and III-V materials which, even for structurally disordered systems like In-Ga-As, still exhibit a constant bowing and a parabolic dependence of the fundamental absorption edge on alloy composition. Second, it is not easily reflected in many band-structure calculations. Most of the time, even if they have been performed in the light of the coherent-potential approximation (CPA), they fail to reproduce such a complicated scheme. As a matter of fact, because of the closer lattice matching achieved in Hg-Cd-Te than in Hg-Zn-Te, these calculations suggest that less deviation (or bowing) from the straight-line average between the two binary compounds should exist in Hg-Cd-Te than in Hg-Zn-Te. In both cases, they predict a parabolic (or nearly parabolic) behavior. This rather large discrepancy between the experimental results and the theoretical calculation is one of the characteristics of MCT. To clear up this point, we have investigated a series of samples with concentrations in the range $x=0.5-1$ (where $x=1$ corresponds to CdTe). We resolve a series of excitonic features and get a clear, unambiguous determination of the first interband transition at different alloy compositions. This gives a constant bowing parameter (i.e., a simple parabolic dependence) with a maximum departure from linearity of 33 meV at $x=0.5$. We discuss these results in the light of the virtual-crystal approximation, using the empirical pseudopotential method, and compare them with recent CPA predictions where both diagonal and off-diagonal disorder terms had been included. We find a surprisingly good agreement which demonstrates, on a purely experimental basis, the near-cancellation of disorder effects expected at the band edge in mercury cadmium telluride.

I. INTRODUCTION

Mercury cadmium telluride (MCT) is a prototype alloy semiconductor which has been investigated for many years.[1] This is the only known system where the band gap energy changes by about 2 eV, running at 2 K from 1.606 eV for CdTe down to -0.303 eV for HgTe (which has inverted Γ_8-Γ_6 ordering) and spans the entire infrared spectrum. For practical reasons most of the experimental research has been concentrated in the far infrared, near the long wavelengths $5-10$ μm (and in the range of cadmium composition $x=0.3-0.2$). This is because of the existence of a large atmospheric window which has proved useful for night detection systems. As a consequence MCT constitutes actually the best standard material for photovoltaic detectors used in this energy range. For totally different reasons, on the theoretical side also, most of the interest focused in the same range of composition (around $x\sim0.16$) but this was because it corresponds to the semiconductor-to-semimetal transition (zero-gap semiconductor).

Concerning the cadmium-rich side of the alloys, much less work has been done, but experimental evidence suggests a breakdown from the virtual-crystal approximation.[2] First Spicer *et al.*[3] performed a series of ultraviolet photoelectron spectroscopic measurements which showed that the density of states associated with the lower-lying valence band could not be accounted for by the simple virtual-crystal approximation (VCA), and that corrections associated with the coherent-potential approximation (CPA) were needed in order to get a better agreement with experimental data. The CPA corrections come from the nonequivalence of cationic Hg and Cd bonds which manifests itself in many different ways. For instance, it is revealed clearly by inspecting the vibrational modes. This was first observed by Vodopyanov *et al.*,[4] who investigated a series of bulk MCT mixed crystals. They have not found evidence for a random distribution of cations (VCA) but, instead, report a tendency to form clusters. This tendency comes directly from the in-

creased weakness of mercury bonds in the presence of foreign (Cd) atoms. With respect to the pure binary compounds, this instability results in mechanical damages, low vacancy-formation energy, and the tendency of atoms to rearrange in order to minimize the crystal total energy.

This breakdown is selective and the point is now to determine how many of the near-band-edge electronic properties are affected by alloying effects. A detailed calculation by Hass *et al.*[5] suggests that mainly the deep *s*-like (cation admixed) valence states are strongly influenced. Since the topmost valence band is almost pure anion *p*-like, one should get no perturbation to the Γ_{8v} states due to cationic disorder. The only contribution of the CPA terms would come through the Γ_{6c} lowest conduction band and should provide direct access to the alloy scattering term. Lastly, depending on whether one is on the HgTe side or the CdTe side, the calculation predicts a fairly complicated dependence on x. The net result is a composition-dependent bowing parameter. Similar results were independently obtained by Wu[6] using a pseudopotential scheme (in both cases a cubic dependence was predicted of which the main reason was alloy disorder) but not by Chen and Sher.[7] They report less bowing using a CPA calculation than they could find using a simple virtual-crystal approximation and argue that only the deep valence states near the zone boundaries, involving a large admixture of cationic *s* states, should be influenced by alloy disorder. From this computation, the difference between the VCA and the CPA results appears particularly small at band edge and no composition-dependent bowing should be expected. The same result was later confirmed in a second calculation[8] where both Hg-Cd-Te and Hg-Zn-Te (MZT) were examined. In both cases a parabolic behavior was expected, with less bowing in the case of MCT as compared with MZT. This is because of the closer lattice matching occurring in the first case and agrees well with standard views on the physics and chemistry of semiconductor alloy systems.

Coming now to the experimental side, the point is to establish clearly which one of these theoretical views agrees best with the experimental results. From the compilation of experimental data, presented by Hansen, Schmit, and Casselman,[9] a nonlinear bowing parameter was suggested. This is because in this work a cubic law was used to fit the energy gap deduced from various experiments, performed at various temperatures. This cubic dependence was first conjectural but later found to agree well with the theoretical results of Refs. 5 and 6. More precise determinations were recently needed, following the report of indirect evidence of alloy disorder effects when analyzing the luminescence emission spectra of a series of Cd-rich samples.[10] Such effects, which suggest that there are in the real space effective potential wells which can bind (localize) free excitons, are difficult to prove. Of course on the microscopic scale they connect with fluctuations of the average lattice potential (VCA) and indicate substitutional disorder, but the binding energy is weak and, to ascertain the existence of localized excitons, one must be able to differentiate them from excitons bound to neutral and/or ionized impurities and from disorder-enhanced polariton structures. This can only be done if the band-gap energy is exactly known, as was clearly demonstrated[11] for the series of II-VI compounds $Cd_{1-x}Zn_xTe$ ($x<0.52$), $CdSe_xTe_{1-x}$ ($x<0.20$), $Zn_{1-x}Mg_xTe$ ($x<0.10$) and $ZnTe_{1-x}Se_x$ ($x<0.05$). In this case the recombination of polariton modes has been found to be predominant over localization effects, while experimental data suggest the opposite for Hg-Zn-Te.[12]

In this work we focus on the experimental determination of the excitonic gap in mercury cadmium telluride by using both reflectivity, absorption and derivative absorption techniques. We find a good agreement between the experimental composition dependence and a simple parabolic law. This agrees well with the theoretical results of Refs. 7 and 8, but contradicts the predictions of Refs. 5 and 6. To establish, on a pure experimental basis, what amount of CPA corrections one has not to worry about when dealing with MCT for device applications, we check our result in the light of current band-structure calculations. We work within the framework of the empirical pseudopotential method (EPM), using a basis of 27 plane waves and the virtual-crystal approximation. Depending on the series of pseudopotential form factors used for cadmium telluride and mercury telluride, we find interesting results: the predicted bowing parameter turns from large and negative (opposite to the experimental findings) to small and positive (in good agreement with the experimental data). Using a recent and well-accepted series of parameters,[13] and performing a careful comparison, we find a VCA contribution at band edge of 0.2 eV. This is of the order of (but slightly larger than) the experimental value (0.132 eV) and gives a strong confirmation that all disorder effects nearly cancel at band edge in mercury cadmium telluride.

II. EXPERIMENTAL TECHNIQUES

We have investigated a series of 11 different samples with concentrations on the cadmium-rich part of MCT. All but one were grown by liquid-phase epitaxy (LPE), using an experimental apparatus already described (see, for instance, Ref. 14). The typical layer thicknesses ranged between 4 and 10 μm and most substrates were bulk CdTe "doped" with 4% zinc. This dilute alloy system, similar to the one associated with the so-called indium-doping of GaAs,[15] resulted in improved layer quality. For comparison purpose, a bulk MCT sample was also used and, in this case, the growth technique[16] was the so-called traveling-heater method (THM). No significant discrepancy could be found between the epitaxial layers and the bulk sample. In both cases the composition was deduced from an ionic microprobe analysis and the corresponding values have been listed in Table I. The standard accuracy is about 0.5% and constitutes the main source of experimental error encountered in this work. This is a rather drastic limitation when working with MCT since the typical change in band-gap energy versus alloy composition is about 20 meV per percent.

To get meaningful data, the low-temperature reflectivity was checked first. The samples were mounted free

TABLE I. Summary of experimental results obtained in this work. At 2 K, clear reflectivity spectra could only be collected in the range $78\% < x < 100\%$. They have been complemented by inspection of the transmission spectra and the first-order derivative of the transmission spectra. All samples used in this work are epitaxial layers of mercury cadmium telluride (MCT) grown by the liquid-phase-epitaxy technique (LPE), except the bulk reference sample grown using the travelling-heater method (THM).

$Hg_{1-x}Cd_xTe$ sample (Growth technique)	Composition $x \pm 0.5$ (%)	E $(n=1)$ (eV)		R (meV)		E_g (eV)	
		Reflectivity	Absorption	Theory	Expt.	Reflectivity	Absorption
MCT 48 (LPE)	100	1.5965		9.5		1.6060	
MCT 83 (LPE)	97.0	1.5315		9.0		1.5405	
bulk (THM)	95.5	1.4992		8.7		1.5079	
MCT 51 (LPE)	92.5	1.4416		8.2		1.4498	
MCT 49 (LPE)	88.0	1.3440	1.3420	7.5	8.0	1.3520	1.3500
MCT 47 (LPE)	78.0	1.1260	1.1435	5.9	6.5	1.1325	1.1500
MCT 56 (LPE)	71.0		1.0130	4.9	6.0		1.0190
MCT 61 (LPE)	71.0		1.0130	4.9	6.0		1.0190
MCT 31 (LPE)	62.0		0.8625	3.8	5.0		0.8675
MCT 67 (LPE)	55.0		0.6980	3.1	3.0		0.7010
MCT 68 (LPE)	50.0		0.6250	2.7	3.0		0.6280

of strain inside a liquid-helium bath, pumped below the λ point, and a high-resolution HRS-2 Jobin-Yvon spectrometer was used. This allowed a practical resolution of $\frac{1}{15000}$. Two different infrared detectors (either a GaAs photomultiplier or a PbS cell, depending on the range of wavelength investigated) have been used and permitted to cover easily the entire composition range. When necessary, the transmission spectrum was also investigated. The sample thickness was first adjusted by chemical etching in a bromine-methanol solution to give a finite transmission value above the absorption edge and then cooled down to liquid-helium temperature. Lastly, since we needed to perform quantitative fits, the spectral response of the full optical system was carefully checked using digital techniques. It was next compared to the experimental reflectivity and/or transmission spectra and used to get calibrated data which allowed us to perform a quantitative comparison with exciton-polariton features in cadmium mercury telluride.

III. EXCITON-POLARITON FEATURES

A. Investigation of the reflectivity spectra

This is the most useful technique in the dilute range of composition $0.8 < x < 1$. Similar to the results already reported for the series of II-IV compounds Cd-Zn-Te, Cd-Se-Te, Zn-Mg-Te and Zn-Se-Te (see Ref. 11, for instance) one resolves clear reflectivity spectra which come from the admixture of photonlike and excitonlike states. This gives new normal modes of the crystal, termed exciton-polaritons.[17] In order to get realistic spectra and compare with experimental data, we compute the polariton dispersion curves by using the standard technique.[18,19] Since for degenerate bands two separate modes propagate in the crystal, one needs an additional boundary condition (ABC) to solve Maxwell equations at the interface. Various ABC's have been introduced but have little effect on the resulting spectra as far as the determination of the transverse energy is concerned. In this work we use ABC2 and suppose the surface, exciton-free (or "dead") layer to have a typical extension of about a Bohr radius.

Versus Γ we get the series of theoretical spectra displayed in Fig. 1(a). Changing the composition from CdTe to HgTe, one expects to increase the broadening parameter and decrease the binding energy. This makes the experimental reflectivity spectra more and more difficult to get. A typical limiting value is $\Gamma/R = 1$. On the experimental side, we could only resolve an exciton-polariton reflectivity structure up to sample MCT 47 (see Table I) which corresponds with the cadmium composition $x = 0.78$. Typical comparisons between theoretical and experimental spectra are shown in Fig. 2 and give all transverse exciton energies listed in Table I.

Using compositions close to $Hg_{0.5}Cd_{0.5}Te$, we could not resolve any more a clear (polaritonic) reflectivity spectrum. This is the case of sample MCT 61. In some cases (samples MCT 56 and 68, for instance) a broad reflectivity structure is found which can be misleading. It does not correlate with any theoretical (polariton) spectra but just comes from a decrease in multiple reflection effects when the absorption coefficient becomes significant. This, of course, appears below the band gap and should not be taken into consideration.

B. Investigation of the transmission spectra

This is the standard technique in the composition range $x < 0.8$. To determine how much of the excitonic features should be again accounted for, we have performed a series of theoretical fits in the light of the three-dimensional theory of direct-allowed excitonic transitions.[20] Of course, to get realistic spectra to compare with the experimental one, we convolute the theoretical expression for $\alpha(E)$ with a Lorentzian function. This is a standard procedure which is now well documented in the literature[21] and will not be discussed further.

The interesting point with MCT is that, changing the composition, one decreases the Rydberg energy and increases the ratio Γ/R. This results in drastic changes in the line shape, as shown in Fig. 1(b). For increasing values of Γ/R it becomes more and more difficult to determine the excitonic absorption edge by just measur-

ing the transmission spectrum and, in this case, we have used a first-order derivative technique to get $d\alpha/dE$. The corresponding theoretical spectra are shown in Fig. 1(c).

In both cases, absorption and derivative absorption, we could get a very satisfactory agreement with experimental data for all samples investigated. This is shown in Fig. 3 for samples MCT 61 ($x=0.71$) and MCT 67 ($x=0.55$). Of course, decreasing the cadmium composition, one decreases the Rydberg energy and the intrinsic excitonic features become less and less resolved, but the extrinsic value of the broadening parameter does not change much versus alloy composition. We find $\Gamma=6$, 6.5, and 5 meV for alloy composition $x=0.88$, 0.71, and 0.55, respectively (see, for instance, Figs. 2 and 3). This is a very interesting point to outline since, increasing the alloy composition, one would also expect to increase the alloy disorder and, then, the broadening parameter Γ. Such a change in broadening parameter has been found for higher-energy-lying interband transitions[22] and correlated with alloy broadening effects. However, it should be noticed that the change is dependent on the critical point investigated: in Ref. 2, both $\Gamma(E_1)$ and $\Gamma(E_1+\Delta_1)$ increase versus alloy composition, and reach a maximum value at about 70% cadmium, while $\Gamma(E_2)$ decreases. In our case the nearly constant value of the broadening parameter demonstrates, on a pure experimental basis, the high quality of our epitaxial layers and confirms the relatively small effect of alloy disorder on the near-band-edge electronic states.

The point is now that, tuning the composition further toward HgTe, one expects the neglect of exciton features to become more and more reasonable. To clear up this point, we compare in Fig. 4 the band-gap energies obtained from two different analysis. First we compute a series of theoretical curves, including excitonic effects and a Lorentzian broadening. This gives $\alpha(E-E_g)$, where E_g is the "true" band-gap energy. Next we plot $\alpha^2(E-E_g)$ versus energy and perform a least mean-square fit through the linear part of the data. This is shown in the inset of Fig. 4 and would give a direct access to the interband edge (labeled E_P) in the case of a parabolic, three-dimensional and nonexcitonic, absorption edge. We find a systematic discrepancy with E_g-E_P depending on the broadening parameter Γ and the Rydberg energy. This is shown in Fig. 4. Roughly speaking, decreasing R we find the parabolic determination to tend to $E_g-\Gamma/2$. With a typical value $\Gamma=6$ meV, this means that in our epitaxial samples the band-gap energies determined in this way should be too low by about 3 meV.

IV. EXPERIMENTAL RESULTS AND COMPOSITION DEPENDENCE OF THE BAND-GAP ENERGY AT 2 K

In Table I we list all experimental results obtained in this work. First we list the cadmium composition and the $n=1$ exciton-polariton transverse frequency (reflectivity and/or transmission data). Then we list theoretical values of the exciton binding energies R.

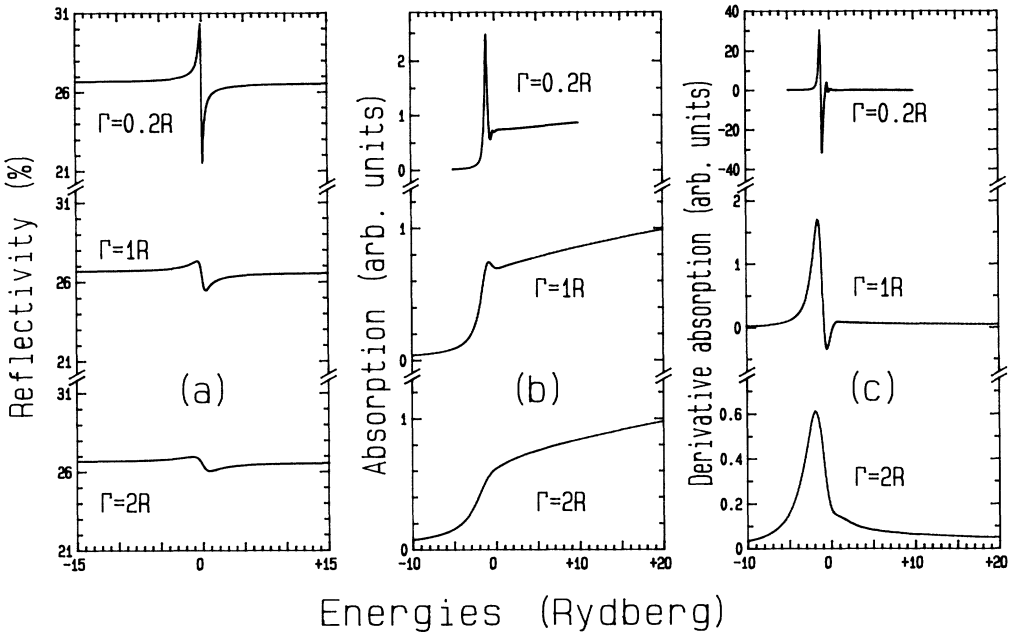

FIG. 1. Changes in the theoretical line shapes expected for various values of Γ/R. The different calculations include excitonic effects and are representative of the range of experimental data collected in this work. (a) Theoretical reflectivity spectra. The dispersion is plotted in this case vs the dimensionless parameter $(E-E_T)/R$ where E_T is the transverse polariton frequency and R the exciton binding energy. (b) Normalized absorption spectra. (c) Derivative absorption. In both cases, for clarity, the dimensionless quantity αd and $d(\alpha d)/dE$ have been plotted vs $(E-E_g)/R$. Now, α is the excitonic absorption coefficient, d the sample thickness, and E_g the true, nonexcitonic, energy gap. All theoretical values of αd have been normalized to unity on the plateau which appears above the fundamental edge.

They come from the simple expression which is only valid in the hydrogenic approximation,

$$R\ (\text{eV}) = 13.6\mu/\epsilon^2\ , \tag{1}$$

where μ is the reduced mass of the exciton and ϵ the static dielectric constant. We take ϵ from the literature[23] and estimate μ from a standard three-band interaction,[1]

$$\mu = \mu_e\mu_h/(\mu_e+\mu_h)\ , \tag{2}$$

where

$$\mu_e^{-1} = 1 + E_P[2/E_g + 1/(E_g+\Delta_{so})]/3 \tag{3}$$

and

$$\mu_h = \text{const} = 0.4\ .$$

To estimate μ_e, we determine E_p from CdTe and get 17.2 eV. Second, from existing band-structure calculations,[7,13,24] we expect linear dependences for the spin-orbit splitting parameter Δ_{so} between the two limiting values[1] $\Delta_{so}(\text{CdTe}) \sim 0.9$ eV and $\Delta_{so}(\text{HgTe}) \sim 1.0$ eV. Lastly, E_g is obtained from the composition dependence

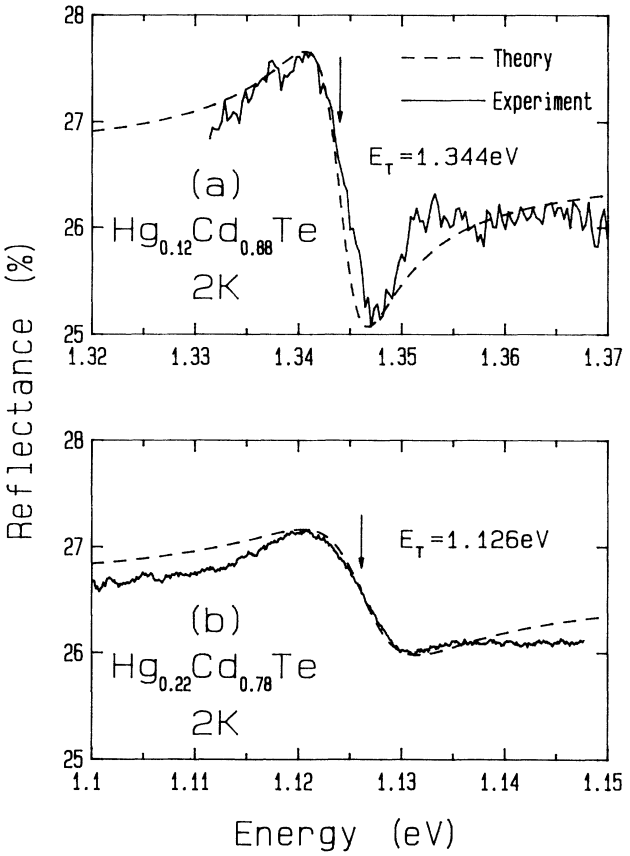

FIG. 2. Experimental reflectivity spectra collected at 2 K on two different samples. In agreement with the theoretical predictions of Fig. 1(a), notice the large change in magnitude associated with the two different spectra: (a) $x=0.88$, $\Gamma=6$ meV and (b) $x=0.78$, $\Gamma=10$ meV. The dashed lines correspond to theoretical fits as discussed in the text. The arrows mark the transverse ($n=1$) exciton-polariton frequencies E_T.

deduced in this work and gives the final values listed in Table I (column 5, under "Theor."). In the case of transmission data, the theoretical values for $\alpha(E)$ depend on both E_g and R at the same time and we had to use self-consistency. Starting from the VCA band gap, we evaluate R but the resulting values have not been listed here. They have been used as starting parameters to perform a preliminary fit on the experimental absorption curves, determine E_g, compute R, and start again. Typical examples of the results obtained in this way have already been shown in Fig. 3. It should be noticed that the final binding energies (listed in column 5, under "Expt.") never depart from the estimated values by more than 10%.

We are now in a position to discuss the composition dependence of the lowest absorption edge. We first start to complement our data near HgTe by using selected values from the literature, listed in Table II. A first one was obtained for $x=0.203$ by McCombe[25] from combined resonance and cyclotron-phonon resonance. The other ones are the results of Guldner *et al.*[26] obtained from magnetoabsorption data at liquid-helium temperature. They cover a fairly large series of samples and have been carefully analyzed. This makes us very confident about the values of the interaction gap reported in this work and we are now dealing with a full series of data. They cover the entire composition range but contradict, in the cadmium-rich side of alloys, the results proposed by Hansen *et al.*[9] We find less experimental bowing than previously reported but, to check the influence of alloy disorder, we attempted a least mean-square fit using the standard assumption of a nonconstant bowing (cubic composition dependence),

$$E_g(x) = A(1-x) + Bx - Cx(1-x) + Dx(0.5-x)(1-x)\ , \tag{4}$$

where

$$A = E_g(\text{HgTe}) = -0.303\ \text{eV}\ ,$$

$$B = E_g(\text{CdTe}) = 1.606\ \text{eV}\ ,$$

and an additional condition, which corresponds to the zero-gap composition

$$E_g(x = 16.5 \pm 0.5) = 0\ ,$$

has been used (see Refs. 26 and 27, for instance).

The results are shown in Fig. 5(a). We find the following.

(i) A very small bowing parameter ($C=0.132$ eV) which corresponds, at composition $x=0.5$, with a deviation from linearity of only 33 meV.

(ii) A negligible value of the cubic contribution (we find $D=0.033$ eV) which gives maximum values at $x=0.25$ and 0.75 of 1.56 meV. This is widely below the experimental accuracy, since a change in composition by only 0.1% would shift the band gap by about 2 meV.

In view of the preceding results, we have attempted a second least mean-square fit assuming now that the bowing parameter was constant and not composition dependent. This gives the results displayed in Fig. 5(b). The

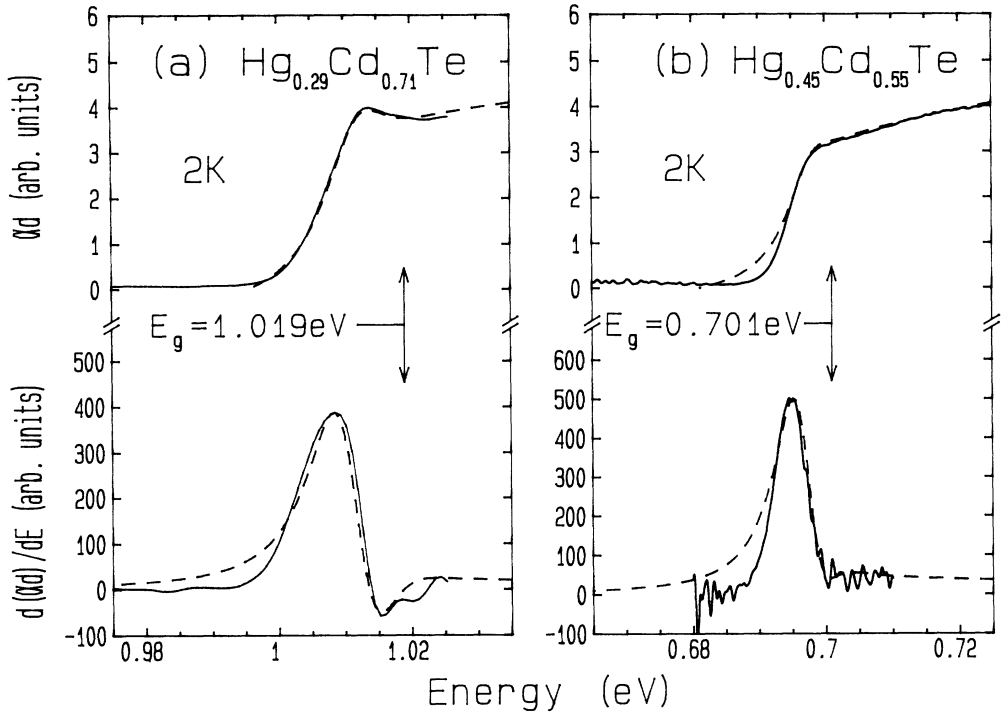

FIG. 3. Experimental absorption and first-order derivative absorption spectra collected at 2 K on two different samples with cadmium compositions: (a) $x=0.71$ and (b) $x=0.55$. Again the dashed lines are theoretical fits using a three-dimensional exciton theory (with $\Gamma=6.5$ and 5 meV, respectively). All quantities are dimensionless and the arrows indicate now the interband, nonexcitonic, absorption edge E_g.

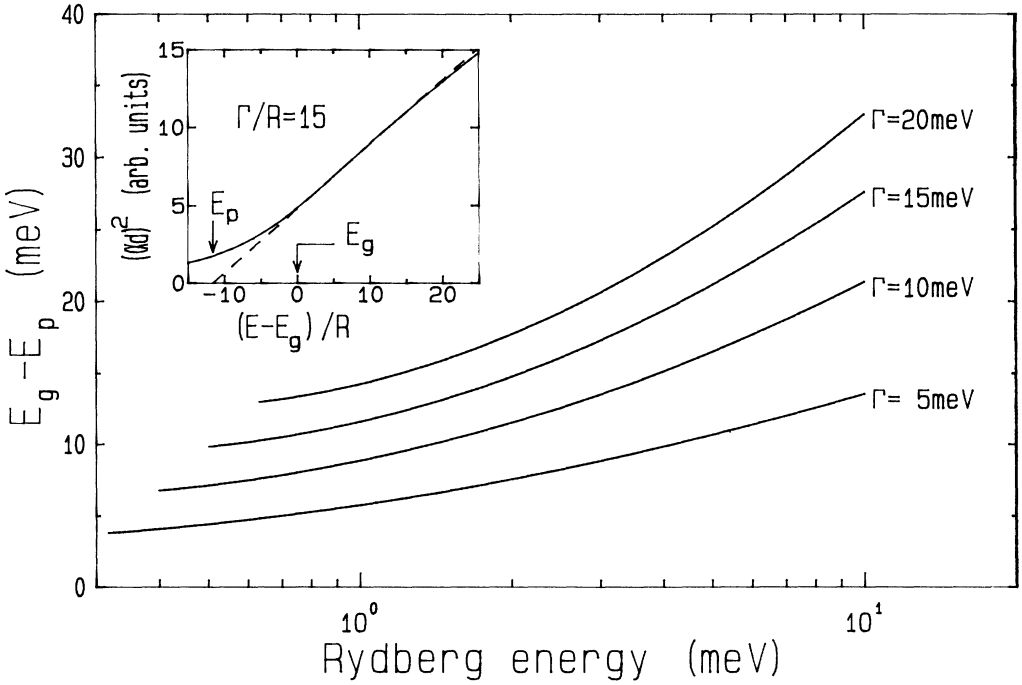

FIG. 4. Comparison of the "parabolic" band edge obtained from the neglect of excitonic features (inset) with the true band-gap energy E_g. We find the energy difference E_g-E_p to be always positive and to decrease vs Rydberg energy. For typical values $\Gamma=6$–10 meV and vanishingly small binding energy, this gives $E_g-E_p\sim 3$–5 meV. This should be kept in mind when discussing transmission data collected on thick samples.

TABLE II. Selected values of the Γ_8-Γ_6 transition near HgTe, obtained from the literature. All data given at liquid-helium temperature.

Cadmium composition (%)	E_g (meV)	Reference
0	−303	26
1	−285	26
2.2	−262	26
4.9	−208	26
11.1	−93	26
13.2	−54	26
14	−34	26
17.6	16	26
20.3	64	25
21.8	83	26
24.8	161	26
26.7	175	26
28.8	212	26

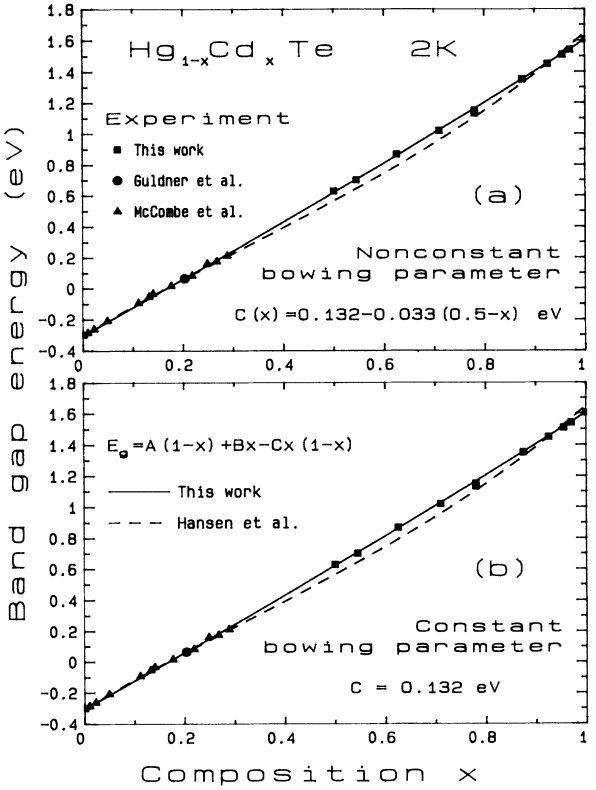

FIG. 5. Composition dependence of the experimental energy gap, as obtained in this work, and comparison with the results obtained by McCombe *et al.* (Ref. 25) or Guldner *et al.* (Ref. 26). Also shown is a compilation of experimental data (dashed line) as obtained from Hansen *et al.* (Ref. 9). (a) shows a least mean-square fit using a composition-dependent bowing, as proposed by Hansen *et al.* (Ref. 9), in agreement with the theoretical results of Hass *et al.* (Ref. 5) or Wu (Ref. 6). We find in this case a vanishingly small contribution of the third-order term (~1.56 meV at maximum amplitude). (b) gives the same results using now a least mean-square fit with a simple parabolic law. We find $C=0.132$ meV.

standard deviation achieved is now 1.77 meV, to be compared with 1.73 meV in the case of Fig. 5(a). The striking conclusion is that one does not need any composition dependence of the bowing parameter to give a satisfactory description of the composition dependence of the lowest absorption edge when dealing with MCT. This is best shown in Fig. 6 where we plot the results of the cubic dependence of Fig. 5(a) against the results of the simple parabolic expression of Fig. 5(b). No significant improvement can be found and we believe that MCT, as far as the lowest band edge is concerned, behaves like a standard pseudobinary alloy and only departs from the linear interpolation by ~30 meV at maximum value. This surprisingly small value should now be compared with the corresponding results reported for the family of II-VI semiconductor alloy systems which crystallize with the cubic structure. This is done in Table III. As far as delocalized states are concerned, we find that our result concerning MCT agrees with the simple idea that the better lattice matching, the smaller bowing parameter. However, as evidenced by modern theories of optical bowing,[28] there is no simple correlation between the lattice mismatch and the nonlinearity of the fundamental edge. Obviously both cationic (Hg-Zn-Te and Cd-Zn-Te) or anionic disorder play an important part, and the larger the change in atomic energies, the larger the bowing. Concerning MCT, we are dealing with an almost ideal situation where both cationic disorder and lattice mismatch (internal strain effects) are small, and the point is now to check how much of our data can be accounted for by the virtual-crystal approximation or come from alloy disorder effects. This is done in Sec. V.

V. OPTICAL BOWING VERSUS VIRTUAL-CRYSTAL APPROXIMATION IN MERCURY CADMIUM TELLURIDE

As already said, many theoretical investigations of the electronic structure of MCT have been published (see, for instance, Refs. 5–8, 13, 24, and references therein) and most calculations agree that at band edge the effect of disorder should be weak. However, they fail to give a unique description of the change in band gap versus alloy composition. To what extent this uncertainty comes from specific problems encountered in MCT with a need for very refined (CPA) descriptions of the alloy system, or lies in a lack of precision when starting from the two binary compounds, should be investigated first.

To clear up this point, we have performed a standard calculation within the empirical pseudopotential method[29] and the virtual-crystal approximation.[30] We first start by selecting an "accurate" set of pseudopotential form factors from the literature. They have been listed in Table IV for CdTe and Table V for HgTe, respectively. Since we are only interested in a good description of the optical properties at band gap, we consider only the calculations which have been carefully fitted to the optical

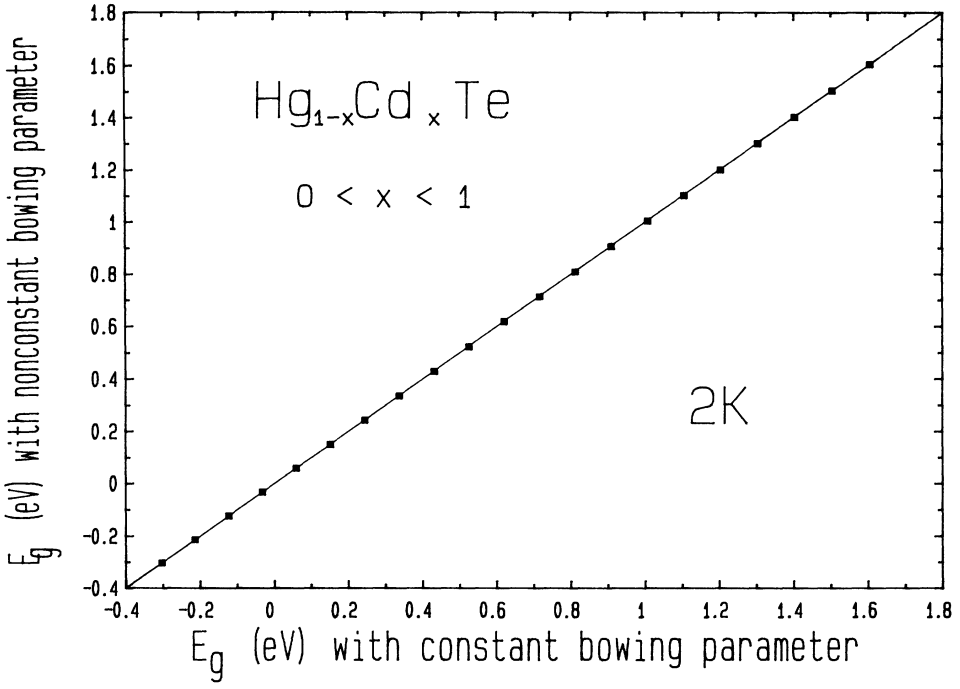

FIG. 6. Comparison of the results of Fig. 5(a) (nonconstant bowing) displayed against the results of Fig. 5(b) (simple parabolic law). No significant improvement could be evidenced in any case.

spectra. This was the case in the work of Ref. 31, where Saravia and Casamayou (SC) considered CdTe and performed a quantitative analysis of both the reflectivity and the photoemission spectra. They could achieve a very satisfactory agreement. Independently, Chadi *et al.*[32] considered both HgTe and CdTe. They computed also theoretical reflectivity spectra which they compared to the optical data. The results appear satisfactory in the case of HgTe but more qualitative in the case of CdTe. Later, Chadi and Cohen[13] repeated the calculation with slightly different form factors and emphasized the density of states in the alloy. All series of parameters are listed in Table IV.

TABLE III. Reported values of the experimental bowing parameter for the family of II-VI semiconductor alloy systems which crystallize with the zinc-blende structure.

II-VI alloy system	Experimental bowing (eV)	Lattice mismatch
Hg-Cd-Te	0.133[a]	3×10^{-3}
Cd-Zn-Te	0.211[b]	6×10^{-2}
Hg-Zn-Te	0.600[c]	6×10^{-2}
Zn-Te-Se	1.266[d]	8×10^{-2}

[a]This work.
[b]G. Neu, A. A. Mbaye, and R. Triboulet, in Ref. 4, p. 1029.
[c]B. Toulouse, R. Granger, S. Rolland, and R. Triboulet, J. Phys. (Paris) **48**, 247 (1987).
[d]A. Ebina, Y. Sato, and T. Takahashi, Phys. Rev. Lett. **32**, 1366 (1974).

Once we know that the best data concerning CdTe are obtained in Ref. 31 and those concerning HgTe in Ref. 32, we compute the change in band-gap energy versus alloy composition. We used[30]

$$V_x(G^2)=x\frac{\Omega_A}{\Omega_x}V_A(G^2)+(1-x)\frac{\Omega_B}{\Omega_x}V_B(G^2)\ ,$$

where $\Omega_A,\Omega_B,\Omega_x$ are unit cells of the pure binary compounds and the alloy, respectively, while $V_A(G^2)$ and $V_B(G^2)$ are pseudopotential form factors for the two binary compounds. To keep the calculation simple and avoid misleading numerical errors, we treat 27 plane waves exactly and, because of the close lattice matching achieved in MCT, neglect all scaling of $V_{A,B}(G^2)$ versus G which would require a fitting procedure and interpolation formulas. This results in the theoretical bowing displayed in Fig. 7 [curve (1)] where the departure from linearity is much too high and has a wrong sign. Repeating the calculation with the set of pseudopotential form factors of Ref. 32, we get essentially the same results, while those of Ref. 13 give the right sign and the right order of magnitude. This clearly demonstrates that small changes in the potential, which might not even alter the band structures, result in drastic changes in the compositional dependence. Such effects have been already reported concerning the temperature dependence of II-VI and

TABLE IV. Selected values of the pseudopotential form factors, extracted from the literature, and used in this work. Also listed are slightly adjusted values to match the band gap of CdTe at 1.606 eV (2 K) using our restricted basis of 27 plane waves and the experimental spin-orbit splitting energy: $\Delta_0=0.927$ eV. [Ref. 1; J. Camassel, D. Auvergne, and H. Mathieu, J. Phys. (Paris) Colloq. **35**, C3-67 (1974).]

CdTe	V_3^S	V_8^S	V_{11}^S	V_3^A	V_4^A	V_{11}^A	V_{12}^A
Ref. 31	−0.202	0.0021	0.04	0.155	0.08	0.04	0
Ref. 32	−0.200	−0.012	0.027	0.168	0.075	0.028	0
Ref. 13	−0.234	−0.042	0.041	0.151	0.068	0.005	0
This work	−0.234	−0.038	0.0428	0.155	0.072	0.001	0

III-V materials[33] but have never been clearly demonstrated for the composition dependence of II-VI (or even III-V) semiconductors.

To go deeper into the details of the various contributions which make such a drastic change possible, we start from HgTe (which is taken common to all calculations) and compute (in eV per rydberg) the series of slope parameters $dE_0/dV(G^2)$ which are listed in Table VI. They just tell us the sensitivity of the band gap in mercury telluride to any given perturbation (in terms of the corresponding change in the pseudopotential form factors). We find that V_{11}, V_8 symmetric and V_3, V_4 antisymmetric are the most sensitive parameters, with a special emphasis on V_{11}^S. We are now in a position to take account of the finite changes in $V(G^2)$ when going from HgTe to CdTe. This is done again in Table VI. All contributions from $\Delta V(G^2)$ to dE_0/dx have been listed, using the set of parameters of Refs. 13, 31, and 32. The interesting point to outline is that a positive departure from linearity (this is the case in Fig. 7 when using the parameters of SC) occurs simply when the theoretical slope at $x=0$ is larger than the experimental average between the two binary compounds. In this case we compute 29 meV per percent, as compared with a linear average of 19 meV per percent. On the opposite, a negative departure from linearity occurs when the initial slope is lower than the linear average; this is the case using the parameter of Chadi and Cohen[13] where we compute 13 meV per percent. Since we know that small changes in the form factors can induce great changes in the composition dependence, we now check our calculation slightly adjusting the parameters to better match at 2 K the band-gap energies of CdTe (1.606 eV) and HgTe (−0.303 eV). The results give $C=0.2$ eV and the composition dependence displayed in Fig. 8 (VCA, this work) against the experimental data.

We should now include CPA corrections and discuss the relative effect of structural disorder.[34] First there exists a random distribution of cation species which is modeled in the tight-binding picture as diagonal disorder. Next comes a subsequent variation in bond length, which corresponds to variations in matrix elements associated with near-neighbor interactions. It is termed nondiagonal disorder. Both types of disorder can shift the VCA band gap in opposite directions and partly cancel, but the main point is that all calculations agree that, in mercury cadmium telluride, the individual contributions are already small at band edge (see, for instance, Refs. 5, 7, and 8). As a matter of fact, we find a very remarkable agreement between our calculation and the CPA results of Ref. 8. This is shown in Fig. 8. Both give "theoretical" bowings of 0.2 and 0.18 eV, respectively and, within theoretical and experimental uncertainty, agree well with the experimental data.

TABLE V. Same as Table IV, but for HgTe. Again the series of adjusted parameters match the band gap at 2 K with $\Delta_0=0.94$ eV (Ref. 32).

HgTe	V_3^S	V_8^S	V_{11}^S	V_3^A	V_4^A	V_{11}^A	V_{12}^A
Ref. 32	−0.262	−0.035	0.05	0.1	0.042	0.02	0.019
This work	−0.262	−0.035	0.0525	0.103	0.042	0.02	0.019

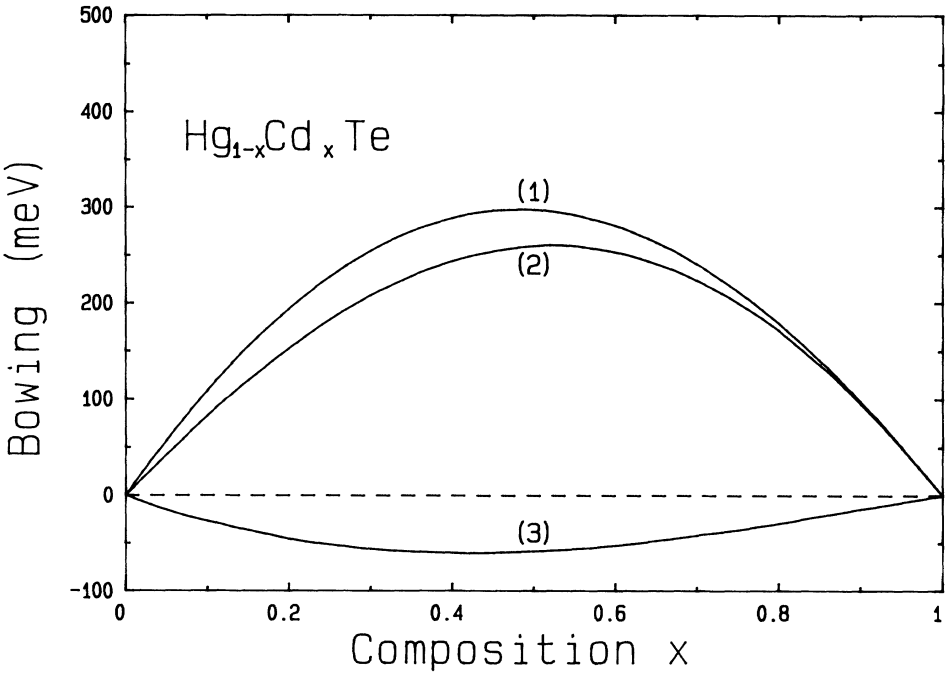

FIG. 7. Theoretical bowing calculated using the empirical pseudopotential method and the virtual-crystal approximation. The pseudopotential form factors from Ref. 32 for HgTe and Refs. 31, 32, and 13 [curves (1), (2), and (3), respectively] for CdTe have been used.

VI. CONCLUSION

We have investigated the composition dependence of the lowest (Γ_8-Γ_6) interband transition in mercury cadmium telluride. At 2 K, we have found a very small (33-meV) departure from linearity which indicates much less disorder effect acting on the carriers than previously thought. Discussing this result in the light of the empirical pseudopotential method and the virtual-crystal approximation, we have found a good agreement with recent pseudopotential form factors but also demonstrated a large sensitivity to the set of parameters used. This establishes that a quantitative prediction of bowing parameters from band-structure calculations is extremely difficult and should be taken cautiously when comparing with experimental data. In a more qualitative way, both our experimental results and the most recent CPA calcu-

TABLE VI. Detail of contributions which add to give near HgTe the initial slope (dE_0/dx) at $x=0$.

HgTe Ref. 30		V_3^S −0.262	V_8^S −0.035	V_{11}^S 0.05	V_3^A 0.1	V_4^A 0.042	V_{11}^A 0.02	V_{12}^A 0.019
$dE_0/dV(G^2)$ (eV/Ry)		0.1	34.3	46	22.6	20.8	−7.6	−9.4
$\Delta V(G^2)$	Ref. 31	0.06	0.0371	−0.01	0.055	0.038	0.02	−0.019
(Ry)	Ref. 32	0.062	0.023	−0.023	0.068	0.033	0.008	−0.019
	Ref. 13	0.028	−0.007	−0.009	0.051	0.026	−0.015	−0.019
Contributions	Ref. 31	6×10^{-3}	1.27	−0.46	1.24	0.79	−0.15	0.18
to dE_0/dx	Ref. 32	6×10^{-3}	0.79	−1.06	1.53	0.68	−0.06	0.18
($x=0$)	Ref. 13	3×10^{-3}	−0.24	−0.41	1.15	0.54	0.11	0.18

[a]Reference 30.
[b]Reference 31.
[c]Reference 32.
[d]Reference 13.

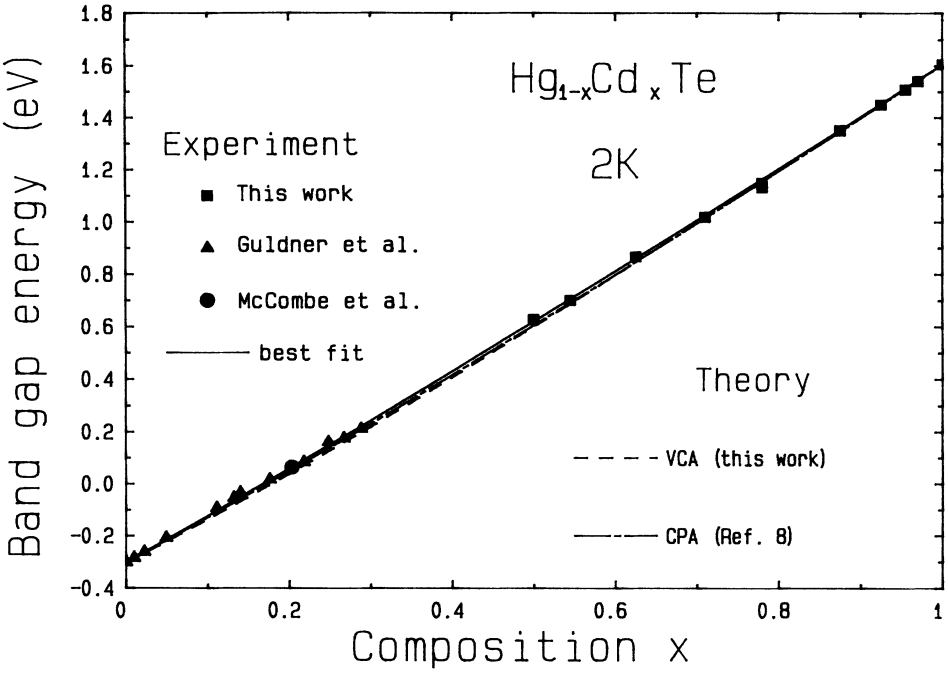

FIG. 8. Comparison of the experimental results obtained in this work with the experimental data of McCombe *et al.* (Ref. 25) and Guldner *et al.* (Ref. 26). In solid line is a least mean-square fit through all experimental data which is compared with the CPA predictions of Ref. 8 (— · — ·) and the simple virtual-crystal approximation (— — —, this work).

lation agree that there is no complicated effect of composition-dependent bowing in the range of technical interest but a simple parabolic departure from linearity. The experimental value of the bowing parameter is small and very close to the one given by the simple VCA approximation. This result, which confirms the conclusion of many band-structure calculations, is evidenced for the first time.

[1]For a recent review concerning MCT, see P. W. Kruse, in *Semiconductors and Semimetals,* edited by R. K. Williardson and A. C. Beer (Academic, New York, 1981), Vol. 18, p. 1; also see M. H. Weiler, *ibid.*, Vol. 16, p. 119.

[2]For a recent review of semiconductor alloy systems, see, for instance, M. Jaros, Rep. Prog. Phys. **48**, 1019 (1985), and references therein.

[3]W. E. Spicer, J. A. Silberman, J. Morgen, I. Lindau, J. A. Wilson, A. B. Chen, and A. Sher, Phys. Rev. Lett. **49**, 948 (1982); W. E. Spicer, J. A. Silberman, I. Lindau, A. B. Chen, A. Sher, and J. A. Wilson, J. Vac. Sci. Technol. A **1**, 1735 (1983).

[4]L. K. Vodopyanov, S. P. Kozyrev, Y. A. Aleschchenko, R. Triboulet, and Y. Marfaing, in *Proceedings of the 17th International Conference on the Physics of Semiconductors, San Francisco, 1984,* edited by D. J. Chadi and W. A. Harrison (Springer-Verlag, New York, 1985), p. 947.

[5]K. C. Hass, H. Ehrenreich, and B. Velicky, Phys. Rev. B **27**, 1088 (1983); H. Ehrenreich and K. C. Hass, J. Vac. Sci. Technol. **21**, 133 (1982).

[6]S. Wu, Solid State Commun. **48**, 747 (1983).

[7]A. B. Chen and A. Sher, J. Vac. Sci. Technol. **21**, 133 (1982).

[8]M. A. Berding, S. Krishnamurthy, A. Sher, and A. B. Chen, J. Vac. Sci. Technol. A **5**, 3014 (1987).

[9]G. L. Hansen, J. L. Schmit, and T. N. Casselman, J. Appl. Phys. **53**, 7099 (1982).

[10]R. Legros, H. Mariette, A. Lusson, and Y. Marfaing (unpublished).

[11]H. Mariette, Y. Marfaing, and J. Camassel, in *Proceedings of the 18th International Conference on the Physics of Semiconductors,* edited by Olof Engström (World Scientific, Singapore, 1987), p. 1405.

[12]H. Mariette, R. Triboulet, and Y. Marfaing, J. Cryst. Growth **86**, 558 (1988).

[13]D. J. Chadi and M. L. Cohen, Phys. Rev. B **7**, 692 (1973).

[14]A. Lusson and R. Triboulet, J. Cryst. Growth (to be published).

[15]J. P. Laurenti, P. Roentgen, K. Wolter, K. Seibert, H. Kurz, and J. Camassel, Phys. Rev. B **37**, 4155 (1987).

[16]R. Triboulet and Y. Marfaing, J. Cryst. Growth **51**, 89 (1981).

[17]J. J. Hopfield and D. G. Thomas, Phys. Rev. **132**, 563 (1963).

[18]D. D. Sell, S. E. Stokowski, R. Dingle, and J. V. Dilorenzo, Phys. Rev. B **7**, 4568 (1973).

[19]H. Mathieu, Y. Chen, J. Camassel, J. Allegre, and D. S. Robertson, Phys. Rev. B **32**, 4042 (1985).

[20]R. J. Elliott, Phys. Rev. **108**, 1384 (1957).

[21]See, for instance, J. Camassel, P. Merle, H. Mathieu, and A. Chevy, Phys. Rev. B **17**, 4718 (1978), and references therein.

[22]L. Viña, C. Umbach, M. Cardona, and L. Vodopyanov, Phys.

Rev. B **29**, 6752 (1984).
[23]R. Dornhaus, G. Nimtz, and W. Richter, Solid State Phys. **78**, 93 (1976).
[24]S. Katsuki and M. Kuninune, J. Phys. Soc. Jpn. **31**, 415 (1971).
[25]B. D. McCombe, R. J. Wagner, and G. A. Prinz, Solid State Commun. **8**, 1687 (1970).
[26]Y. Guldner, C. Rigaux, A. Mycielski, and Y. Couder, Phys. Status Solidi B **82**, 149 (1977).
[27]S. H. Groves, T. C. Harman, and C. R. Pidgeon, Solid State Commun. **9**, 451 (1971).
[28]A. Zunger and J. E. Jaffe, Phys. Rev. Lett. **51**, 662 (1983).
[29]F. Bassani, in Ref. 1, Vol. 1, p. 21.
[30]D. Richardson, J. Phys. C **4**, L289 (1971).
[31]L. R. Saravia and L. Casamayou, J. Phys. Chem. Solids **33**, 145 (1972).
[32]D. J. Chadi, J. P. Walter, M. L. Cohen, Y. Petroff, and M. Balkanski, Phys. Rev. B **5**, 3058 (1972).
[33]J. Camassel and D. Auvergne, Phys. Rev. B **12**, 3258 (1975).
[34]K. C. Hass, R. J. Lempert, and H. Ehrenreich, Phys. Rev. Lett. **52**, 77 (1984).